are diffusion limited but the reactions of Cl⁻, AcO⁻,[23b] and probably SO_4^{2-} with **2** are slower than diffusion.

(3) The stepwise preassociation mechanism predicts a limiting reaction velocity at high nucleophile concentrations when essentially all of the substrate exists in the encounter complex [Nu⁻·R-X] with the nucleophile (Scheme I). This provides an explanation for the downward curvature that is observed in the plots of k_{obsd} against the concentration of nucleophile for the reaction of azide ion and thiocyanate ion with **1-I** (Figure 2).

Figure 5 shows a replot of the data for N_3^- from Figure 2 according to eq 3 which was derived for Scheme III. Scheme

$$k_{obsd} - bk_{solv}[N_3^-] = \frac{k_{solv} + k_{Nu}K_{as}[N_3^-]}{1 + K_{as}[N_3^-]} \quad (3)$$

III is a simplified version of Scheme I in which k_{solv} is the observed first-order rate constant for solvolysis of **1-I**, K_{as} is the association constant for formation of the substrate–nucleophile encounter complex, and k_{Nu} is the macroscopic first-order rate constant for conversion of this encounter complex to the nucleophile adduct. The left-hand side of eq 3 is the observed rate constant for the reaction of **1-I** corrected for the negative specific azide ion salt effect that is observed at high [NaN₃] (Figure 2). The specific azide ion salt effect on the reaction of **1-I** (by k_1, Scheme I) and the reaction of the preassociation complex [N₃⁻·**1-I**] (by k_1', Scheme I) were assumed to be the same as that on the reaction of **1-Br** for which $b = -0.104$ (Figure 3). The value of $k_{solv} = 4.0 \times 10^{-3}$ s⁻¹ (Table II) was used to obtain a nonlinear least-squares fit of the data to eq 3 (solid line, Figure 5), which gave $K_{as} = 0.67$ M⁻¹ and $k_{Nu} = 8.0 \times 10^{-3}$ s⁻¹.

The values for K_{as} and k_{Nu} obtained from this analysis are reasonable. A value of $K_{as} = 0.3$ M⁻¹ has been estimated for formation of an encounter complex between 1-propanethiol and 1-(4-methylphenyl)ethyl chloride in 50:50 trifluoroethanol/water.[7] The somewhat larger value of $K_{as} = 0.67$ M⁻¹ estimated here could refect stabilizing electrostatic interactions between the azide anion

and the positive end of the dipole of the CF₃ group at [N₃⁻·**1-I**].

The ratio $k_{Nu}/k_{solv} = 2$ requires that the reaction of **1-I** in the encounter complex with azide ion be 2-fold faster than in the presence of solvent alone. Most or all of this difference must be due to the more favorable partitioning of [N₃⁻·**2**·I⁻] than of [**2**·I⁻] to products ($k_2 > k_{-d}$, Scheme I). There is no evidence for a significant difference between k_1 and k_1', so nucleophilic assistance to the reaction of **1-I** is minimal.

The large Grunwald–Winstein values of $m = 1.3$ and 1.2 for the solvolysis reaction of **1-I** and the apparent bimolecular substitution reaction of azide ion with **1-I**, respectively, are consistent with similar changes in polarity on moving from the ground state to the transition state for these reactions. A detailed evaluation of data for reactions in mixed methanol/water solvents with respect to a stepwise preassociation mechanism would require additional experiments at higher concentrations of azide ion (see Figure 5), which are not feasible because of the limited solubility of sodium azide in aqueous/organic solvents.

Summary. These experiments provide a relatively simple protocol for determining if kinetically bimolecular nucleophilic substitution reactions proceed through a carbocation reaction intermediate. The reactions of nucleophilic anions with **1-X** are kinetically second order in nucleophile only when the reactions of *both* the nucleophile and the leaving group anion with the free carbocation **2** are diffusion limited. This is consistent with a stepwise preassociation mechanism for the bimolecular substitution reaction. The relative rate acceleration observed at [Nucleophile] = 1.00 M is small (≤40%, Figure 2 and Table II), even for those reactions which particularly favor the observation of a stepwise bimolecular substitution reaction. These results suggest that large rate accelerations should not be expected for nucleophilic substitution reactions in water which follow the stepwise preassociation reaction mechanism.

Evaluation of Potential Ferromagnetic Coupling Units: The Bis(TMM) Approach to High-Spin Organic Molecules

S. Joshua Jacobs, David A. Shultz, Rakesh Jain, Julie Novak, and Dennis A. Dougherty*

Contribution No. 8728 from the Arnold & Mabel Beckman Laboratories of Chemical Synthesis, California Institute of Technology, Pasadena, California 91125. Received September 17, 1992

Abstract: Four new hydrocarbon tetraradicals, **1–4**, each composed of two triplet trimethylenemethane (TMM) subunits linked by a potential ferromagnetic coupling unit (FC), were synthesized and characterized by variable-temperature electron paramagnetic resonance (EPR) spectroscopy. Simulation of the EPR powder spectra and a priori calculation of the zero-field splitting parameters aided spectral assignment. The Heisenberg Hamiltonian appears to quantitatively model relative spin-state energies in **1–4**. In three cases ferromagnetic coupling was achieved, as evidenced by quintet ground states in the resulting tetraradicals. In one case, strong evidence for antiferromagnetic coupling was obtained.

Introduction

A key to the rational design of magnetic organic materials is the ability to control spin–spin coupling of unpaired electrons.[1,2] One approach we have been pursuing is shown schematically in

Figure 1a. We conceptually divide a high-spin material into two components: the spin-containing fragment (SC), which provides the unpaired electrons, and the ferromagnetic coupling unit (FC).[3,4]

(1) *Magnetic Molecular Materials*; Gatteschi, D., *et al.*, Eds.; Kluwer Academic Publishers: The Netherlands, 1991; pp 105–120. Buchachenko, A. L. *Russ. Chem. Rev. Engl. Transl.* **1990**, *59*, 307. Proceedings of the Symposium on Ferromagnetic and High Spin Based Materials, 197th National Meeting of the American Chemical Society, Dallas, TX, April 9–14, 1989; Miller, J. S., Dougherty, D. A., Eds. *Mol. Cryst. Liq. Cryst.* **1989**, *176*, 1.

(2) (a) Iwamura, H. *Adv. Phys. Org. Chem.* **1990**, *26*, 179. (b) Dougherty, D. A. *Acc. Chem. Res.* **1991**, *24*, 88.

(3) (a) Dougherty, D. A. *Mol. Cryst. Liq. Cryst.* **1989**, *176*, 25. (b) Novak, J. A.; Jain, R.; Dougherty, D. A. *J. Am. Chem. Soc.* **1989**, *111*, 7618. (c) Dougherty, D. A. *Pure Appl. Chem.* **1990**, *62*, 519. (d) Dougherty, D. A.; Kaisaki, D. A. *Mol. Cryst. Liq. Cryst.* **1990**, *183*, 71. (e) Kaisaki, D. A.; Chang, W.; Dougherty, D. A. *J. Am. Chem. Soc.* **1991**, *113*, 2764. (f) Dougherty, D. A.; Grubbs, R. H.; Kaisaki, D. A.; Chang, W.; Jacobs, S. J.; Shultz, D. A.; Anderson, K. K.; Jain, R.; Ho, P. T.; Stewart, E. G. In *Magnetic Molecular Materials*; Gatteschi, D., *et al.*, Eds.; Kluwer Academic Publishers: The Netherlands, 1991; pp 105–120.
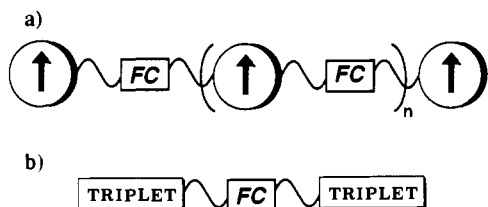
Ferromagnetic Coupling Units: The Bis(TMM) Approach

J. Am. Chem. Soc., Vol. 115, No. 5, 1993 1745

a)

b)

Figure 1. (a) General design of high-spin assemblies. (b) Design of quintet ground-state tetraradicals.

Table I. Biradicals Substructures in Compounds **1–4**

biradical	$\Delta E_{ST}(kcal/mol)^a$	$|D/hc|$ (cm^{-1})
5	10^{5p}	0.011^{6u}
6	1.7^{5l-n}	$0.112^{b,6e,f}$
7	$0.9^{5l,m,o}$	$0.084^{6c,d}$
8	-1.3^{c}	$-^{12,13}$
9	15^{5q}	0.026^{7}

^{a} From ab initio calculations. ^{b} D for 1,3-dimethyl-1,3-cyclo-butanediyl. ^{c} Present work.

A general FC is a structure that will high-spin (ferromagnetically) couple any two SCs, regardless of the structural details of the SC. There are many options in choosing an SC. From our perspective, the more challenging element is the FC.

In the present work, we evaluate four potential FCs using tetraradicals **1–4**. Of course, one can identify candidate FCs by
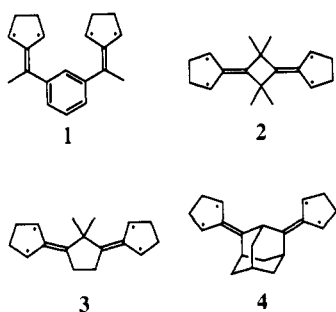
considering organic biradicals that have triplet ground states.[5,6]

Figure 2. Heisenberg energy level diagrams for two interacting triplet biradicals.
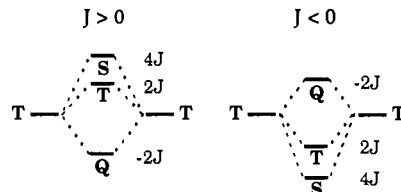

Figure 2. Heisenberg energy level diagrams for two interacting triplet biradicals.

In effect, one can think of a triplet biradical as being composed of two simple radicals (the SCs) linked through an FC. Table I shows the biradicals that correspond to the FCs we study here. Our goal is to test the generality of such FCs by using triplet biradicals as the SCs (Figure 1b). As described below, this substantially complicates the spin system and allows for a more stringent evaluation of an FC.

In each tetraradical, the SC is a triplet 2-alkylidene-1,3-cyclopentanediyl[7] (**9**, Table I). This derivative of the prototypical delocalized triplet ground-state biradical trimethylenemethane (TMM)[3a,b] has been developed extensively by Berson. We consider it an ideal SC because of its large triplet preference, synthetic accessibility, and thermal stability in rigid media (up to 300 K).

Four different FCs are probed: m-phenylene;[8,9] 1,3-cyclo-butane;[5l,n,6e–g] 1,3-cyclopentane;[5o,6c,d,10,11] and 1,3-cyclohexane[12,13] locked into a chair conformation by an adamantane skeleton. If an FC is successful in this tetraradical context, the ground state should be a quintet (**Q**). Using this approach, we have found that

(4) We do not claim to be the first or only group to consider the problem in this way. The famous polycarbene work was the first example of such a design (see below). The explicit and more general schematic of Figure 1 has, however, proved very useful to us.

(5) (a) Borden, W. T., Ed.; *Diradicals*; Wiley: New York, 1982. (b) Salem, L.; Rowland, C. *Angew. Chem., Int. Ed. Engl.* **1972**, *11*, 92. (c) Dauben, W. G.; Salem, L.; Turro, N. *J. Acc. Chem. Res.* **1975**, *8*, 41. (d) Borden, W. T.; Davidson, E. R. *Acc. Chem. Res.* **1981**, *14*, 69. (e) Wirz, J. *Pure Appl. Chem.* **1984**, *56*, 1289. (f) Bonacic-Koutecky, V.; Koutecky, J.; Michl, J. *Angew. Chem., Int. Ed. Engl.* **1987**, *26*, 170. (g) Klein, D. J.; Nelin, C. J.; Alexander, S.; Matsen, F. A. *J. Chem. Phys.* **1982**, *77*, 3101. (h) Lahti, P. M.; Ichimura, A. S. *J. Org. Chem.* **1991**, *56*, 3030. (i) Ovchinnikov, A. A. *Theor. Chim. Acta* **1978**, *47*, 297. (j) Borden, W. T.; Davidson, E. R. *J. Am. Chem. Soc.* **1977**, *99*, 4587. (k) Longuett Higgins, H. C. *J. Chem. Phys.* **1950**, *18*, 265. (l) Goldberg, A. H.; Dougherty, D. A. *J. Am. Chem. Soc.* **1983**, *105*, 284. (m) Doubleday, C., Jr.; McIver, J. W., Jr.; Page, M. *J. Am. Chem. Soc.* **1982**, *104*, 6533. (n) Pranata, J.; Dougherty, D. A. *J. Phys. Org. Chem.* **1989**, *2*, 161. (o) Conrad, M.; Pitzer, R.; Schaefer, H., III. *J. Am. Chem. Soc.* **1979**, *101*, 2245–2246. See, however: Dowd, P.; Chang, W.; Paik, Y. H. *J. Am. Chem. Soc.* **1986**, *108*, 7416; **1987**, *109*, 5284. Du, P.; Borden, W. T. *J. Am. Chem. Soc.* **1987**, *109*, 930. (p) Kato, S.; Morokuma, K.; Feller, D.; Davidson, E. R.; Borden, W. T. *J. Am. Chem. Soc.* **1983**, *105*, 1791. (q) Hood, D. M.; Schaefer, H. F., III; Ptizer, R. M. *J. Am. Chem. Soc.* **1978**, *100*, 8009–8010. Dixon, D. A.; Dunning, T. H., Jr.; Eades, R. A.; Kleier, D. A. *J. Am. Chem. Soc.* **1981**, *103*, 2878–2880.

(6) (a) Dowd, P. *J. Am. Chem. Soc.* **1966**, *88*, 2587. (b) Dowd, P. *J. Am. Chem. Soc.* **1972**, *94*, 1066. (c) Buchwalter, S. L.; Closs, G. L. *J. Am. Chem. Soc.* **1975**, *97*, 3857. (d) Buchwalter, S. L.; Closs, G. L. *J. Am. Chem. Soc.* **1979**, *101*, 4688. (e) Jain, R.; Snyder, G. J.; Dougherty, D. A. *J. Am. Chem. Soc.* **1984**, *106*, 7294. (f) Jain, R.; Sponsler, M. B.; Coms, F. D.; Dougherty, D. A. *J. Am. Chem. Soc.* **1988**, *110*, 1356. (g) Sponsler, M. B.; Jain, R.; Coms, F. D.; Dougherty, D. A. *J. Am. Chem. Soc.* **1989**, *111*, 2240. (h) Snyder, G. J.; Dougherty, D. A. *J. Am. Chem. Soc.* **1989**, *111*, 3927. (i) Rule, M.; Matlin, A. R.; Seeger, D. E.; Hilinski, E. F.; Dougherty, D. A.; Berson, J. A. *Tetrahedron* **1982**, *38*, 787. (j) Rule, M.; Matlin, A. R.; Hilinski, E. F.; Dougherty, D. A.; Berson, J. A. *J. Am. Chem. Soc.* **1979**, *101*, 5098. (k) Seeger, D. E.; Hilinski, E. F.; Berson, J. A. *J. Am. Chem. Soc.* **1981**, *103*, 720. (l) Inglin, T. A.; Berson, J. A. *J. Am. Chem. Soc.* **1986**, *108*, 3394. (m) Matlin, A. R.; Inglin, T. A.; Berson, J. A. *J. Am. Chem. Soc.* **1982**, *104*, 4954. (n) Goodman, J. L.; Peters, K. S.; Lahti, P. M.; Berson, J. A. *J. Am. chem. Soc.* **1985**, *107*, 276. (o) Gisin, M.; Rommel, E.; Wirz, J.; Burnett, M. N.; Pagni, R. M. *J. Am. Chem. Soc.* **1979**, *101*, 2216. (p) Platz, M. S. *J. Am. Chem. Soc.* **1979**, *101*, 3398. (q) Platz, M. S.; Carrol, G.; Pierrat, F.; Zayas, J.; Auster, S. *Tetrahedron* **1982**, *38*, 777. (r) Platz, M. S.; Burns, J. R. *J. Am. Chem. Soc.* **1979**, *101*, 4425. (s) Muller, J.-F.; Muller, D.; Dewey, H. J.; Michl, J. *J. Am. Chem. Soc.* **1978**, *100*, 1629. (t) Fisher, J. J.; Michl, J. *J. Am. Chem. Soc.* **1987**, *109*, 583. (u) Wright, B. B.; Platz, M. S. *J. Am. Chem. Soc.* **1983**, *105*, 628.

(7) (a) Berson, J. A. *Acc. Chem. Res.* **1978**, *11*, 446. (b) Berson, J. A. In ref 2a, pp 151–194.

(8) (a) Itoh, K. *Chem. Phys. Lett.* **1967**, *1*, 235. (b) Wasserman, E.; Murray, R. W.; Yager, W. A.; Trozzolo, A. M.; Smolinsky, G. *J. Am. Chem. Soc.* **1967**, *89*, 5076.

(9) (a) Nakamura, N.; Inoue, K.; Iwamura, H.; Fujioka, T.; Sawaki, Y. *J. Am. Chem. Soc.* **1992**, *114*, 1484. (b) Ishida, T.; Iwamura, H. *J. Am. Chem. Soc.* **1991**, *113*, 4238. (c) Fujita, I.; Teki, Y.; Takui, T.; Kinoshita, T.; Itoh, K. *J. Am. Chem. Soc.* **1990**, *112*, 4074. (d) Iwamura, H. *Pure Appl. Chem.* **1987**, *59*, 1595. (e) Tukada, H.; Mutai, K.; Iwamura, H. *J. Chem. Soc., Chem. Commun.* **1987**, *15*, 1159. (f) Iwamura, H. *Pure Appl. Chem.* **1987**, *58*, 187. (g) Sugawara, T.; Bandow, S.; Kimura, K.; Iwamura, H.; Itoh, K. *J. Am. Chem. Soc.* **1986**, *108*, 368. (h) Takui, T.; Itoh, K. *Chem. Phys. Lett.* **1973**, *120*. (i) Teki, Y.; Takui, T.; Itoh, K.; Iwamura, H.; Kobayashi, K. *J. Am. Chem. Soc.* **1983**, *105*, 3722. (j) Sugawara, T.; Bandow, S.; Kimura, K.; Iwamura, H.; Itoh, K. *J. Am. Chem. Soc.* **1984**, *106*, 6449.

(10) (a) Coms, F. D.; Dougherty, D. A. *Tetrahedron Lett.* **1988**, *29*, 3753. (b) Coms, F. D.; Dougherty, D. A. *J. Am. Chem. Soc.* **1989**, *111*, 6894. (c) Adam, W.; Grabowski, S.; Platsch, H.; Hannemann, K.; Wirz, J.; Wilson, R. M. *J. Am. Chem. Soc.* **1989**, *111*, 6896.

(11) (a) Coms, F. D. Ph.D. Thesis, California Institute of Technology, Pasadena, CA, 1990. (b) Stewart, E. G. Ph.D. Thesis, California Institute of Technology, Pasadena, CA, 1992.

(12) The preparation of the bicyclic diazene precursors to 1,3-cyclohexanediyl and 1,3-dimethyl-1,3-cyclohexanediyl has been reported: Wilson, R. M.; Rekers, J. W.; Packard, A. B.; Elder, R. C. *J. Am. Chem. Soc.* **1980**, *102*, 1633. However, no report on the biradicals has been published.

(13) Photolysis of the azo precursor of 2,4-adamantanediyl gave no EPR signal: Dowd, P.; Chang, W. Personal communication.

Scheme I[a]
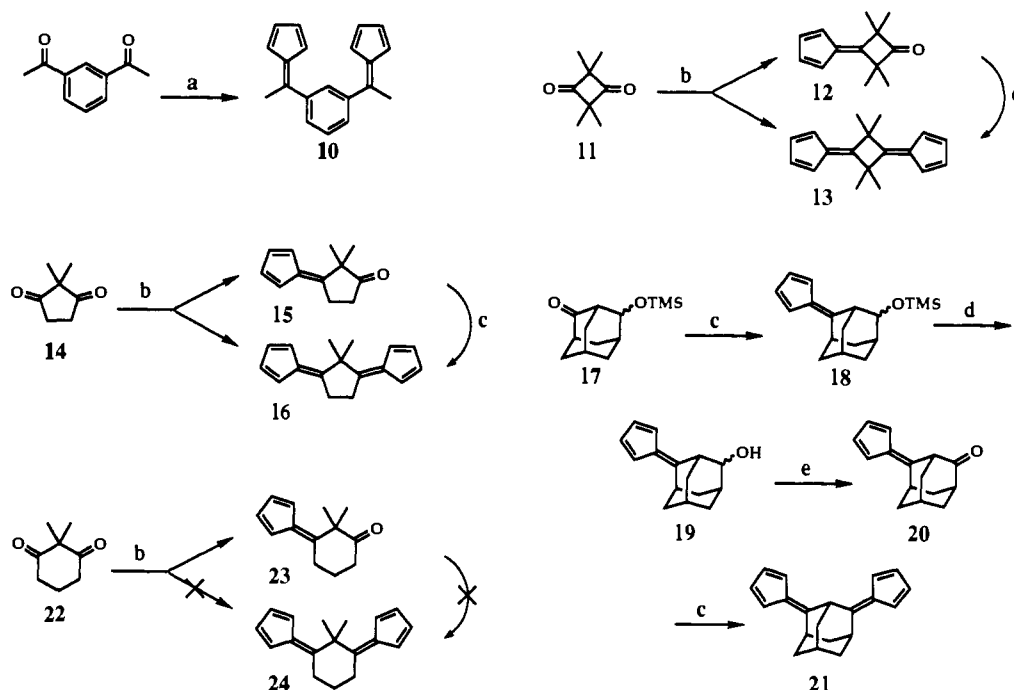
[a] Reaction conditions: (a) cyclopentadiene, pyrrolidine, MeOH; (b) CpLi, BF₃·Et₂O, THF; (c) CpMgBr; (d) Et₃N·3HF, CH₃CN; and (e) oxalyl chloride, DMSO, CH₂Cl₂; NEt₃, CH₂Cl₂.

the first three candidates are indeed FCs, although 1,3-cyclopentane is a very weak FC. In contrast, 1,3-cyclohexane is an antiferromagnetic coupling unit. These studies have provided useful insights into the spin preferences of tetraradicals and, by inference, the simple biradicals that correspond to the FCs. We have also been able to test *quantitative* models, both for spin-state orderings and for EPR spectral parameters, and have found them to be quite useful in a predictive sense for structures such as **1–4**. We believe the bis(TMM) strategy typified by **1–4** will provide a powerful, general approach to evaluating FCs.[14]

Results

Model. A tetraradical is distinguished by four electrons in four nearly degenerate nonbonding molecular orbitals. These give rise to 70 possible electronic configurations, which can be assigned to 36 states: 20 singlets (S), 15 triplets (T), and one quintet (Q). In a hydrocarbon tetraradical, ionic states are expected to be high-lying, leaving only the six covalent states: two singlets, three triplets, and one quintet.[15] The situation is simplified further if the biradical subunits are "robust triplets",[2b] i.e., if the singlet–triplet gap (ΔE_{ST}) is large enough that at any reasonable temperature only the triplet state of the biradical is measurably populated. In this case, T + T coupling is responsible for the low-energy states of the tetraradical, which then number only three: a quintet, a triplet, and a singlet. Thus, judicious choice of components in executing the design of Figure 1b reduces the complexity of constructing tetraradicals with quintet ground states. The TMMs we have employed as SCs have ΔE_{ST} values of ca.

15 kcal/mol[5q] and so satisfy the "robust triplet" criterion.

The interaction of the two T subunits can be modeled by the Heisenberg Hamiltonian.[16,17] This spin-only Hamiltonian (eq 1) is defined in terms of the individual spin operators of the interacting subunits and a magnetic exchange parameter, J. The J term embodies all of the spatial information of the wave function, i.e., the through-space and through-bond interactions which actually determine the ground-state spin preference. Representative tetraradical eigenfunctions are given in eqs 2–4, and the energies, E_S, of tetraradical states with total angular momentum S are given in eq 5 and Figure 2. A potential FC can thus be fully characterized by its value of J: if $J > 0$, high-spin, or ferromagnetic, coupling occurs and Q is the ground state; while if $J < 0$, low-spin, or antiferromagnetic, coupling occurs and S is the ground state. By synthesizing and studying structures such as **1–4**, we can determine the sign, and in favorable cases the magnitude, of J of different potential FCs.

$$\hat{H} = -2J\hat{S}_1 \cdot \hat{S}_2 \tag{1}$$

$$Q = |1\rangle|1\rangle \tag{2}$$

$$T = 2^{-1/2}(|1\rangle|0\rangle - |0\rangle|1\rangle) \tag{3}$$

$$S = 3^{-1/2}(|1\rangle|-1\rangle - |0\rangle|0\rangle + |-1\rangle|1\rangle) \tag{4}$$

$$E_S = -J(S(S + 1) - 4) \tag{5}$$

Synthesis. Bisdiazenes were employed as photochemical precursors to tetraradicals. Bisdiazenes **1**-(N₂)₂-**4**-(N₂)₂ were prepared from bisfulvenes (Scheme I). Bisfulvene **10** was prepared by the condensation of diacetylbenzene, cyclopentadiene, and pyrrolidine in methanol.[18a] All 1,3-cyclopentanediones yielded acyclic bisfulvenes under these conditions, and upon reaction with standard organometallic reagents (CpLi/CpNa, CpMgBr[19]) as well, due to retroaldol ring opening of the intermediate β-ox-

(14) For other quintets and related very high spin structures, see: (a) Rajca, A.; Utamapanya, S.; Thayumanavan, S. *J. Am. Chem. Soc.* **1992**, *114*, 1884. (b) Utamapanya, S.; Rajca, A. *J. Am. Chem. Soc.* **1991**, *113*, 9242. (c) Rajca, A.; Utamapanya, S.; Xu, J. T. *J. Am. Chem. Soc.* **1991**, *113*, 9235. (d) Rajca, A. *J. Org. Chem.* **1991**, *56*, 2557. (e) Rajca, A. *J. Am. Chem. Soc.* **1990**, *112*, 5890. (f) Rajca, A. *J. Am. Chem. Soc.* **1990**, *112*, 5889. (g) Seeger, D. E.; Lahti, P. M.; Rossi, A. R.; Berson, J. A. *J. Am. Chem. Soc.* **1986**, *108*, 1251 (correction, p 6100). (h) Murata, S.; Sugawara, T.; Iwamura, H. *J. Am. Chem. Soc.* **1987**, *109*, 1266. (i) Murata, S.; Iwamura, H. *J. Am. Chem. Soc.* **1991**, *113*, 5547. (j) Kirste, B.; Grimm, M.; Kurreck, H. *J. Am. Chem. Soc.* **1989**, *111*, 108. (k) Tukada, H.; Mutai, K. *J. Chem. Soc., Chem. Commun.* **1991**, *109*, 35. (l) Baumgarten, M.; Müller, U.; Bohnen, A.; Müllen, K. *Angew. Chem., Int. Ed. Engl.* **1992**, *31*, 448.

(15) See, for example: McElwee-White, L.; Goddard, W. A.; Dougherty, D. A. *J. Am. Chem. Soc.* **1984**, *106*, 3461.

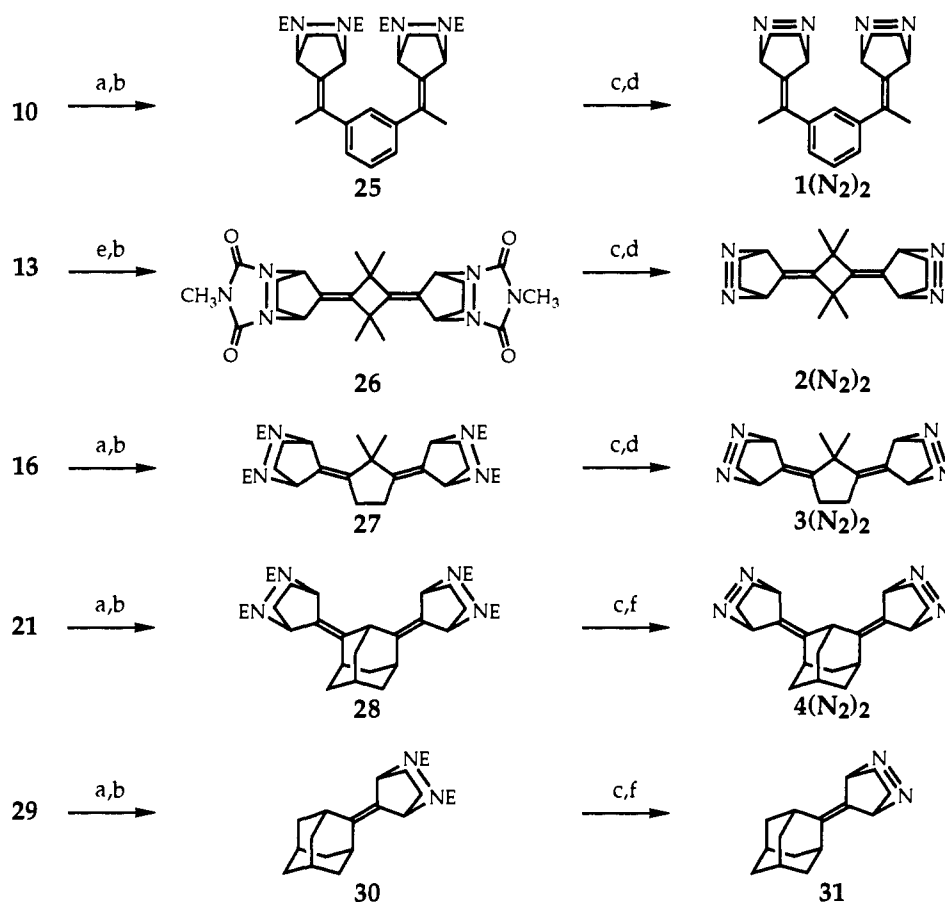(16) Itoh, K. *Pure Appl. Chem.* **1978**, *50*, 1251.

(17) (a) Carlin, R. L. *Magnetochemistry*. Springer Verlag: Berlin, 1986; p 123 ff. (b) Kittel, C. *Introduction to Solid State Physics*, 6th ed.; Wiley: New York, 1986; p 426.

(18) (a) Stone, K. J.; Little, R. D. *J. Org. Chem.* **1984**, *49*, 1849. (b) Little, R. D.; Carroll, G. L.; Petersen, J. L. *J. Am. Chem. Soc.* **1983**, *105*, 928.

(19) Stille, J. R.; Grubbs, R. H. *J. Org. Chem.* **1989**, *54*, 434.

Scheme II[a]

[a] Reaction conditions: (a) DMAD, CH_2Cl_2; (b) $KO_2CN=NCO_2K$, AcOH, CH_2Cl_2; (c) KOH, *i*-PrOH, Δ, $NaHCO_3$; (d) NiO_x, CH_2Cl_2; (e) MTAD, hexanes/Et_2O; and (f) $CuCl_2$, NH_4OH. E = CO_2Me.

oalkoxide. We have found that the inclusion of the strong Lewis acid $BF_3·Et_2O$ in the reaction of CpLi with a 1,3-cycloalkanedione in THF suppresses the ring-opening reaction and leads directly to bisfulvenes.[20] Generally, the fulvene ketones (**12, 15, 23**) are produced in greater yield, and they can be transformed into the bisfulvenes by reaction with CpMgBr.[19] The results are summarized in Scheme I. Although the yields are low, this simple procedure is expedient, in that it provides adequate amounts of material rapidly. We have found this route more convenient than previously published routes to **13**.[3b,21]

The methyl groups blocking the 2-positions, which were necessary in order to avoid problems with enolization, completely suppressed formation of **24**, presumably due to steric effects. Thus, for a cyclohexane-based FC, we turned to the adamantane system, and bisfulvene **21** could easily be prepared from **17**, the TMS ether of known 8-hydroxy-2-adamantanone (Scheme I).[22]

The elaboration of bisfulvenes **10, 13, 16**, and **21** into bisdiazenes proceeded via a standard sequence (Scheme II). Two equivalents of dimethyl azodicarboxylate (DMAD) add in Diels–Alder fashion to **10, 16**, and **21**, but DMAD does not add to **13**. Fortunately, the more reactive dienophile *N*-methyltriazolinedione (MTAD) reacts with **13** to give the desired double-addition product. Reduction of the endocyclic olefinic linkages in these adducts with diimide[18b] provided compounds **25–28** as mixtures of diastereomers. Hydrolysis with KOH in refluxing *i*-PrOH and oxidation with NiO_x or $CuCl_2/NH_3$ gave bisdiazenes **1-(N_2)$_2$-4-(N_2)$_2$**.[6f]

EPR Spectroscopy of High-Spin Molecules. A brief review of quintet- and triplet-state EPR spectroscopy will assist in the

interpretation of the experimental spectra.[23] For a quintet (triplet) there are five (three) sublevels with m_s = 0, ±1, ±2 (m_s = 0, ±1). These levels are energetically distinct even in the absence of an external magnetic field due to a dipolar coupling among (between) the electron spins. This coupling is described by a zero-field splitting (zfs) tensor, $\tilde{D}$, which is characteristic of a particular species. The $\tilde{D}$ tensor is represented by two scalar parameters in the EPR Hamiltonian, D and E, which can be deduced from the observed spectra.

EPR selection rules allow four (two) Δm_s = 1 transitions. In the randomly oriented samples under consideration, only molecules with one of their principal $\tilde{D}$ tensor axes nearly aligned with the external magnetic field will contribute significantly to the first-derivative EPR spectrum. There are then 4 × 3 = 12 (2 × 3 = 6) lines which might be detected. Total spectral width is $6D$ (2D), and at X-band ($\approx$9.27 GHz) the line widths in the quintet spectra described here are large enough in comparison with D that fewer than 12 lines are observed. Additionally, the small D values in these systems preclude the occurrence of off-axis extra lines, which have been used to assign EPR spectra in other cases.[24] The practical effect of these factors is to complicate assignment of the observed spectra to a quintet spin state.

A formally forbidden "half-field" Δm_s = 2 transition is also observed in the spectra of quintet and triplet states due to the relaxation of EPR selection rules by the zfs; a large zfs leads to a greater intensity of the transition. We observe distinct lines in this region for some quintets. This feature of quintet spectra is a useful diagnostic probe, especially in the present systems, in which triplets are converted slowly into quintets by photolysis.

(20) This combination of reagents was inspired by a report on the stability and oxophilic nature of mixtures of *n*-BuLi and $BF_3·Et_2O$: Eis, M. J.; Wrobel, J. E.; Ganem, B. *J. Am. Chem. Soc.* **1984**, *106*, 3693.
(21) Freund, W.; Hünig, S. *Helv. Chim. Acta* **1987**, *70*, 929.
(22) Faulkner, D.; McKervey, M. A. *J. Chem. Soc. C* 1971, 3906.

(23) Weltner, W., Jr. *Magnetic Atoms and Molecules*; Dover Publications, Inc.: New York, 1983; pp 256–265.
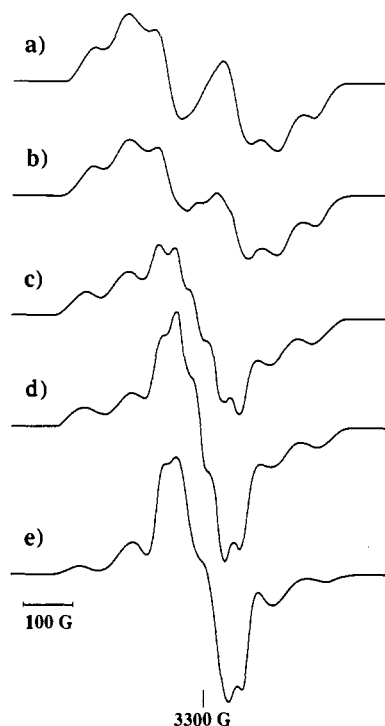(24) Teki, Y.; Takui, T.; Itoh, K. *J. Chem. Phys.* **1988**, *88*, 6134.

Figure 3. EPR spectra obtained from photolysis of 1-$(N_2)_2$ at 77 K and (a) 15-, (b) 90-, (c) 450-, and (d) 900-min $h\nu$. (e) Simulated quintet with $|D|/hc = 0.0076$ cm^{-1} and $|E|/hc = 0.0003$ cm^{-1}.

In addition to these basic spectral features, we have two powerful tools to assist in the spin–state assignment of EPR spectra. The first is a complete simulation of the powder spectrum.[25] The effective EPR spin Hamiltonian used in the simulations is

$$\hat{H} = g\beta\mathbf{B}\cdot S + D(S_z^2 - (S(S+1)/3)) + E(\hat{S}_x^2 - \hat{S}_y^2) \quad (6)$$

in which terms of fourth order and higher in $\hat{S}$ are neglected and an isotropic g is assumed. Details of this calculation are given in the Experimental Section.

Our assignments are also substantially bolstered by the ability to predict D values for the spin states of a tetraradical composed of two coupled triplet biradicals. We have applied the relations among zero-field splitting tensors in such systems (eqs 7 and 8),

$$\tilde{D}^Q = \frac{\tilde{D}^A + \tilde{D}^B}{6} + \frac{\tilde{D}^{AB}}{3} \quad (7)$$

$$\tilde{D}^T = -\frac{\tilde{D}^A + \tilde{D}^B}{2} + \tilde{D}^{AB} \quad (8)$$

which have been presented by Itoh.[16,26,27] In eqs 7 and 8 $\tilde{D}^A$ ($\tilde{D}^B$) is the $\tilde{D}$ tensor of the A (B) biradical; in the present case, A = B. We assumed axial symmetry for the biradical fragments, since the biradical E values are small. Calculation of the tetraradical $\tilde{D}$ tensors then depended on the values of D of the constituent biradicals, and on selecting an appropriate common coordinate system. The D values of the pertinent biradical subunits are listed in Table I. $\tilde{D}^{AB}$ is not simply $\tilde{D}$ of the coupling unit, because there is not a full spin on the carbons which the FC connects. For this reason, $\tilde{D}^{AB}$ was scaled by the Hückel spin densities of the biradical subunits at these carbons.[8a,28] It is worth emphasizing that $\tilde{D}^A$,

(25) Bonomo, R. P.; Di Bilio, A. J.; Riggi, F. *Chem. Phys.* **1991**, *151*, 323.

(26) Rose, M. E. *Elementary Theory of Angular Momentum*; Wiley: New York, 1957.

(27) A detailed derivation of the results of eqs 7 and 8 has been reported: Scaringe, R. P.; Hodgson, D. J.; Hatfield, W. E. *Mol. Phys.* **1978**, *35* (3), 701–713.
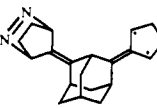
Table II. Observed Zfs Parameters for Monoazo Triplet Biradcials
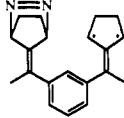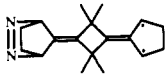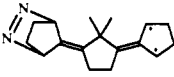
species	$|D/hc|$(cm^{-1})	$|E/hc|$(cm^{-1})
1(N_2)	0.0205	0.0023
2(N_2)	0.0256	0.0044
3(N_2)	0.0254	0.0035
4(N_2)	0.0252	0.0039

Table III. Predicted and Experimental D Values for Tetraradicals

species	$D^A(=D^B)/hc$ (cm^{-1})	D^{AB}/hc (cm^{-1})	$|D^Q/hc|$(cm^{-1}) calcd	$|D^Q/hc|$(cm^{-1}) exptl	$|D^T/hc|$(cm^{-1}) calcd	$|D^T/hc|$(cm^{-1}) exptl
1	0.020	0.0053	0.0078	0.0076	0.029	
2	0.026	−0.049	0.020	0.021	0.037	
3	0.026	−0.037	0.016	0.018	0.030	0.036
4	0.026	−0.031^a	0.015		0.028	

^{a} Calculated by scaling values from 6 and 7 by the distance calculated for 8 using a $1/r^3$ relationship. See refs 6e,f and 10a.

$\tilde{D}^B$, and $\tilde{D}^{AB}$ are obtained directly from experimental measurements of appropriate biradicals, and these are thus truly *a priori* predictions of the zfs values for the quintet and triplet states of tetraradicals **1–4**.

EPR Results. Solutions of individual bisdiazenes were frozen at cryogenic temperatures, and photochemical extrusion of N_2 was effected by irradiation of the diazene n–π^* chromophore. Initial photolysis of 1-$(N_2)_2$-4-$(N_2)_2$ produced EPR spectra whose carriers were easily and unambiguously identified as triplet TMMs.[6a,b,7] Further photolysis altered the EPR spectra, producing noticeable differences between the initial and final spectra.

Figure 3a shows the EPR spectrum obtained upon initial photolysis of 1-$(N_2)_2$ in MTHF at 77 K. The six lines in the $\Delta m_s = 1$ region and the $\Delta m_s = 2$ transition (not shown) identify the carrier of the EPR signal as the triplet biradical 1-(N_2) (Table II). The zero-field splitting parameters for this biradical are $|D|/hc = 0.0205$ cm^{-1} and $|E|/hc = 0.0023$ cm^{-1}, in accord with values reported by Berson for similar molecules.[7] Figure 3b–d shows the evolution of the recorded EPR spectra as this sample was subjected to further photolysis. The spectrum obtained after extended photolysis is well reproduced by computer simulation, shown in Figure 3e, employing a quintet Hamiltonian with $S = 2$, $|D|/hc = 0.0076$ cm^{-1}, and $|E|/hc = 0.0003$ cm^{-1}. We therefore assign this spectrum to quintet **1**, ^{5}**1**.

Initial EPR spectra obtained after compounds 2-$(N_2)_2$-4-$(N_2)_2$ were irradiated are shown in Figures 4a, 5a, and 6a. Each is

(28) The scaling factor for the zfs calculations (eqs 7 and 8) is $^2/_3$, because this is the total spin density on these carbons, and the method combines $\tilde{D}$ tensors of the intact biradicals. However, for energy evaluation using the Heisenberg Hamiltonian (eq 1), the relevant quantity is the fraction of the total spin of the biradical involved in the interaction, which is $^1/_3$. Note that for both types of calculations we assume a planar π system. This seems reasonable for **2–4**, but for **1** we have evidence for significant twisting (S. K. Silverman, unpublished results). A full discussion of this issue will be presented elsewhere.
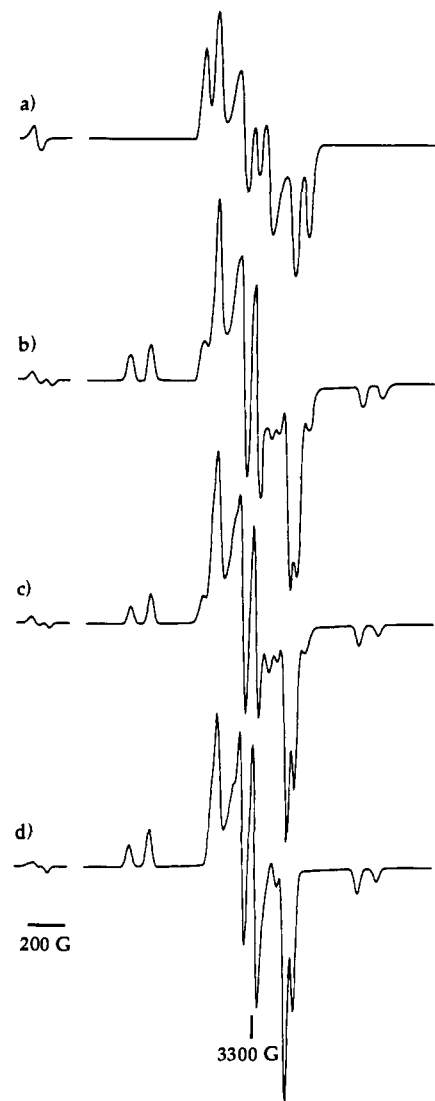
a)

b)

c)

d)

200 G

3300 G

Figure 4. EPR spectra obtained after (a) 30-s photolysis of 2-(N₂)₂ at 70 K, assigned to ^{3}2-(N₂), and (b) 353-min photolysis of 2-(N₂)₂ at 70 K, assigned to a mixture of ^{3}2-(N₂) and ^{5}2. (c) Mixture of simulations of ^{3}2-(N₂) and ^{5}2 spectra (see spectrum d) representing a 1:1 molar ratio. (d) Simulation of spectrum of ^{5}2 with zfs parameters $|D|/hc$ = 0.0207 cm⁻¹ and $|E|/hc$ = 0.0047 cm⁻¹.

typical of a TMM,[7] and the signal carriers are assigned as 2-(N₂)-4-(N₂). The zfs parameters of these triplet biradicals are listed in Table II. Figure 4b shows the EPR spectrum obtained after extended photolysis of a sample of 2-(N₂)₂ in MTHF at 70 K. We assign the new fine structure peaks to ^{5}2, with $|D|/hc$ = 0.0207 cm⁻¹ and $|E|/hc$ = 0.0047 cm⁻¹. A simulation of a quintet spectrum with these parameters is shown in Figure 4c. Comparison of the spectra in parts b and c of Figure 4 reveals that formation of 2 is incomplete and some triplet 2-(N₂)₂, ^{3}2-(N₂), remains in the matrix. A sum of simulated spectra representing a 1:1 mixture of ^{3}2-(N₂) and ^{5}2 (Figure 4d) matches the experimental spectrum exactly. Analogous spectra from the extended photolysis of 3-(N₂)₂ in MTHF at 4 K are shown in Figure 5b–d; for ^{5}3, $|D|/hc$ = 0.0178 cm⁻¹ and $|E|/hc$ = 0.0047 cm⁻¹. Our spectral assignments are thoroughly consistent with the D values of ^{5}1, ^{5}2, and ^{5}3 calculated from eq 7 (Table III).

In contrast to the results for 2-(N₂)₂ and 3-(N₂)₂, when 4-(N₂)₂ is irradiated for a prolonged period at either 4 or 77 K, no new fine structure appears. During an extended photolysis period, the amplitude of the observed triplet signal decreases (Figure 6b,c). The intensity of the EPR signal resulting from irradiation of 4-(N₂)₂ was measured as a function of photolysis time. In separate experiments, MTHF solutions of monodiazene 31 and 4-(N₂)₂ were irradiated at 50 K. For the conversion of 31 to the corre-

a)

b)

c)

d)

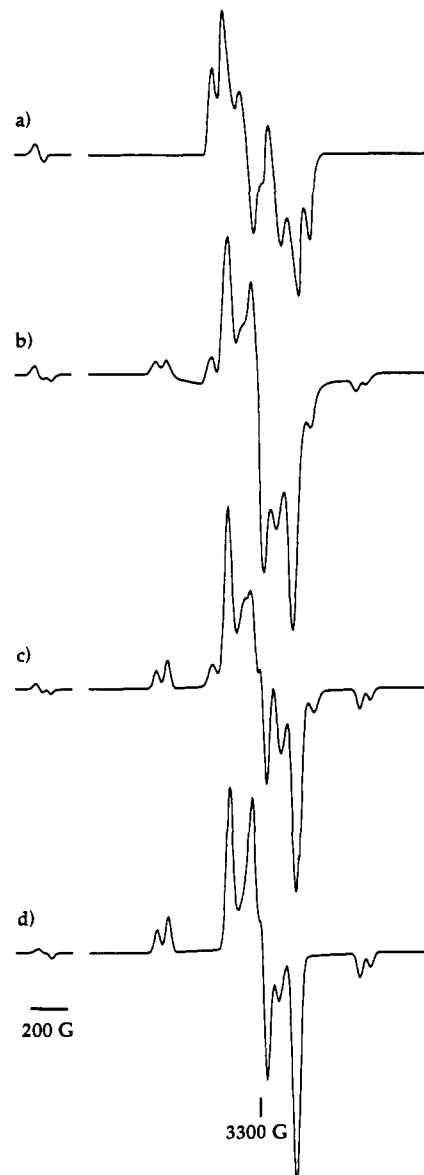200 G

3300 G

Figure 5. EPR spectra obtained after (a) 60-s photolysis of 3-(N₂)₂ at 4 K, assigned to ^{3}3-(N₂), and (b) 650-min photolysis of 3-(N₂)₂ at 4 K, assigned to a mixture of ^{3}3-(N₂) and ^{5}3. (c) Mixture of simulations of ^{3}3-(N₂) and ^{5}3 spectra (see spectrum d) representing a 1:1 molar ratio. (d) Simulation of spectrum of ^{5}3 with zfs parameters $|D|/hc$ = 0.0178 cm⁻¹ and $|E|/hc$ = 0.0047 cm⁻¹.

sponding biradical 32, first-order growth of the triplet signal is observed (k_A = 0.015 min⁻¹) with a very slight decay upon extended photolysis (k_D = 2 × 10⁻⁵ min⁻¹) (Figure 7). The intesity profile of the EPR signal from the photolysis of 4-(N₂)₂ (Figure 7) strongly suggests that the carrier of this signal is the first product in a two-step unimolecular decomposition (k_1 = 0.004 min⁻¹, k_2 = 0.011 min⁻¹).[29] From these results, we conclude that the extended photolysis of 4-(N₂)₂ produces tetraradical 4, but that 4 is EPR silent because it has a *singlet* ground state. Of course, it is conceivable that photodecomposition of 4-(N₂) differs in some way from that of the large number of related, previously studied structures,[7] but we consider this possibility highly unlikely.

Variable-Temperature Studies. The quintet states of tetraradicals 1–3 are all readily observed at temperatures as low as 3.8 K, strongly suggesting a quintet ground state in each case. Monitoring signal intensity as the temperature is raised can provide information on the energetic magnitude of this preference. Tetraradical 1 is quite stable thermally, and raising the tem-

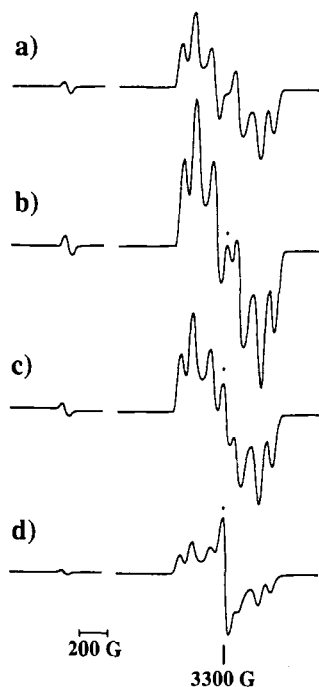(29) Atkins, P. W. *Physical Chemistry*, 4th ed.; Freeman: New York, 1990; p 798.

Figure 6. EPR spectra resulting from photolysis of 4-$(N_2)_2$ at 77 K. Irradiation times: (a) 30 min, (b) 190 min, (c) 300 min, and (d) 607 min. All spectra were recorded at the same receiver gain setting. A small doublet impurity is marked with an asterisk.
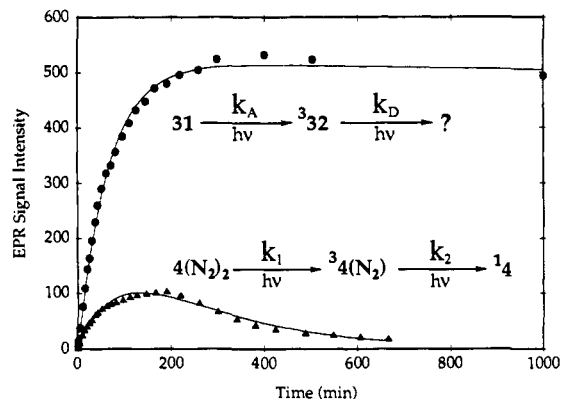

Figure 7. Plot of EPR signal intensity vs photolysis time at 50 K for 3**1** and 4-$(N_2)_2$.

perature as high as 135 K (1,2-propanediol matrix) produces only intensity changes consistent with conventional Curie behavior. Thus the preference for a quintet ground state in **1** is at least 1350 cal/mol (see eq 12, below).

When samples of **2** in 1,2-propanediol are warmed, Curie behavior is also observed, but only up to 85 K. At this temperature, the signals due to ^{5}**2** disappear over a period of a few minutes.[6f,8] A similar irreversible decay of ^{5}**3** signals is seen at temperatures above 120 K.

However, when samples of **3** in 1,2-propanediol are observed in the 4–100 K range, two new peaks symmetrically displaced from the center of the $\Delta m_s = 1$ region appear in the higher temperature spectra. A spectrum recorded at 40 K is shown in Figure 8. These changes are reversible; the new peaks completely disappear upon recooling. Thus ^{5}**3** is in thermal equilibrium with an EPR-active species. By reference to the state energy diagram of Figure 2, the obvious candidate for the EPR active species is ^{3}**3**. As computed from eq 8 and shown in Table III, ^{3}**3** should have $|D|/hc$ = 0.036 cm^{-1}. If the two new peaks correspond to the outer lines of a triplet spectrum, then $|D|/hc$ = 0.030 cm^{-1} for the triplet species. We consider such agreement compelling and conclude that ^{5}**3** is in equilibrium with ^{3}**3** and ^{1}**3**. Plotting the change in the observed triplet signal intensity vs temperature (Figure 9)

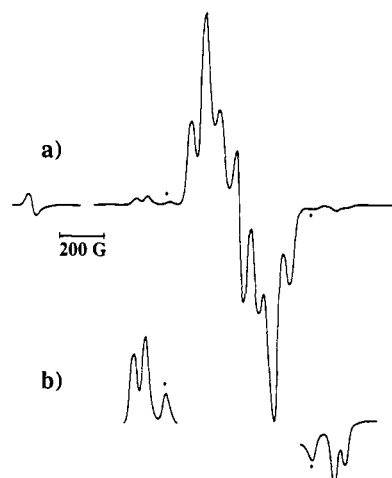**Figure 8.** EPR spectra of Figure 5b recorded at 40 K (a) with a normal gain setting and (b) with the gain increased 10×. Asterisks mark peaks due to ^{3}**3**.
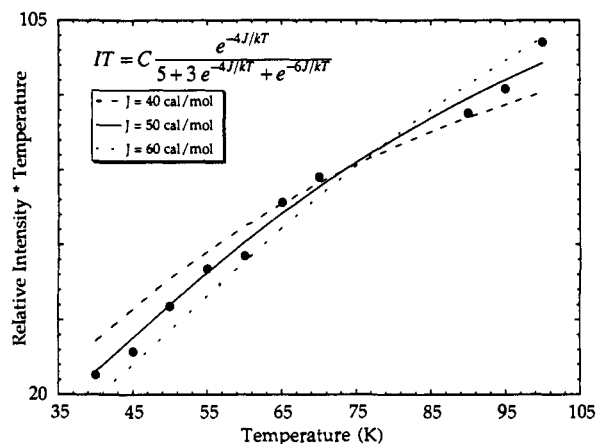

Figure 9. Plot of IT (the product of relative EPR signal intensity and temperature) vs T for ^{3}**3**. The curves shown for different J values are the best fits of the data to the equation shown, which incorporates both Boltzmann and Curie effects.

allows us to estimate J as 50 cal/mol, and so the energy separation between ^{5}**3** and ^{3}**3** is ΔE_{QT} = 200 cal/mol.

We have found that the spin-state energies of the tetraradicals can be reconciled with ab initio calculations of the singlet–triplet gaps (ΔE_{ST}) in the corresponding biradicals. Modeling a biradical with the Heisenberg Hamiltonian (eq 1)gives $2J$ as the S–T gap (eq 9). This J transfers directly to a bis(TMM), except it must be scaled by $(1/3)(1/3) = ^1/_9$ since only $^1/_3$ of the total TMM spin density is on the FC carbons.[28] Combining this factor with eq 5 gives eq 10. Combining eqs 9 and 10 gives eq 11, relating the Q–T gap of a bis(TMM) to the S–T gap of the biradical that corresponds to the FC.

$$\Delta E_{ST} = 2J \qquad (9)$$

$$\Delta E_{QT} = 4J/9 \qquad (10)$$

$$\Delta E_{QT}/\Delta E_{ST} = ^2/_9 \qquad (11)$$

$$\Delta E_{QT}/kT \leq 5.0 \qquad (12)$$

For cyclopentanediyl, ΔE_{ST} = 900 cal/mol (J = 450 cal/mol) has been calculated.[5o] Application of eq 11 predicts that ΔE_{QT} = 200 cal/mol in **3**, in remarkable agreement with experiment. Certainly the agreement is fortuitous to some extent, as the calculated S–T gap has some uncertainty and spin polarization effects in the TMM unit have been ignored. Using the S–T gaps of Table I, Q–T gaps of 2200 cal/mol for **1** and 380 cal/mol for **2** are obtained. Our experience with ^{3}**3** shows that one can expect to observe the excited T state when eq 12 is satisfied. For **1**, this

Ferromagnetic Coupling Units: The Bis(TMM) Approach

J. Am. Chem. Soc., Vol. 115, No. 5, 1993 1751

requires a temperature of 222 K, precluding observation of ^{3}**1** in the matrices employed to date ($T < 140$ K). The temperature range in which ^{3}**2** might be observable is quite close to where irreversible thermal decay sets in.

We have computed ΔE_{ST} for trimethylene at a geometry analogous to **4**. This geometry was obtained by MM2 geometry optimization of bisfulvene **24**, followed by isolation of the desired three-carbon fragment and attachment of hydrogens at the optimized bond and dihedral angles, but at normal C–H bond lengths (1.10 Å). This trimethylene has a 1.3 kcal/mol preference for a *singlet* ground state at the same level of theory[51,o] used for the other biradicals discussed above. The results of these calculations are completely consistent with our previous model concerning the origin of the spin-state energy differences, which emphasizes the role of through-bond coupling, the importance of the C1–C2–C3 angle, and the C1–C3 distance.[51,m] This computed ΔE_{ST} is, of course, consistent with the apparent singlet ground state of tetraradical **4**.

Summary and Conclusions

The scope of *m*-phenylene as a ferromagnetic coupling unit has been expanded. Previous efforts have focused primarily on one-center spin-containing units such as carbenes and simple radicals.[8,9,14] The quintet ground state of **1** establishes that delocalized biradicals are also ferromagnetically coupled by this unit. In other work, we have shown that *m*-phenylene also serves as an FC for localized biradicals.[30] Our work directed toward the "polaronic ferromagnet" has established that radical cations are also ferromagnetically coupled by *m*-phenylene.[3e] Thus, this FC appears to have broad potential in the design of high-spin and potentially magnetic materials.[31]

The results on **2–4** allow several conclusions concerning potential "localized"[6f] FCs. On the basis of the results for **2**, 1,3-cyclobutane appears to be an effective FC. The thermal instability of **2** above 85 K could signal a liability in this unit, but further work will be required to quantify the effect. In contrast, the results for **3** and **4** indicate that 1,3-cyclopentane is a fairly weak ferromagnetic coupling unit, and 1,3-cyclohexane (chair) is an *anti*ferromagnetic coupling unit. Thus, neither seems well-suited to producing very high spin arrays or magnetic materials.

An encouraging aspect of our findings is the remarkable success of eqs 7 and 8[16,26,27] in predicting zfs values for tetraradicals, and the equivalent performance of eq 11 in predicting state energy orderings for **3**. The quantitative nature of these predictions will facilitate study of a wide array of tetraradical structures.

A few comments about the "bis(TMM)" approach might also be appropriate. First, it must be emphasized that, conceptually, the strategy is directly analogous to the polycarbene approach that has been so brilliantly exploited by Itoh, Iwamura, and others.[2a,8,9] There are some practical advantages to the bis(TMM) approach. First, the "Berson" TMMs we have used are less reactive than diaryl carbenes, especially with regard to H-atom abstraction from matrices.[32] Second, there is more design flexibility with this approach, in that biscarbene analogues of **2–4** would be unrealistic targets. Finally, the quantitative modeling of the bis(TMM) compounds described above opens the way for many further studies of tetraradicals. The results on **2–4** demonstrate that the bis-(TMM) approach can also provide information about simple biradicals. This includes information that would be difficult to obtain from direct studies of the biradicals themselves, either because the biradicals are not thermally stable (**3** vs **7**) or because the biradicals themselves have never been observed (**4** vs **8**). Further studies along these lines are in progress.

Experimental Section

General. Unless otherwise noted, reactions were run under an atmosphere of dry argon or nitrogen. Tetrahydrofuran, diethyl ether, dioxane,

and benzene were distilled from sodium benzophenone ketyl. Methylene chloride and acetonitrile were distilled from CaH_2. TLC was performed on 0.25-mm silica precoated glass plates visualized under UV light and/or with vanillin stain. Flash chromatography[33] was performed on 230–400-mesh silica gel. EI mass spectra data, 70 eV, were obtained on a Hewlett-Packard 5890/5970 GC/MS. High-resolution mass spectral analyses were performed by the Mass Spectral Facility at the University of California, Riverside. NMR spectra were obtained on JEOL GX-400, GE QE-300, or Varian EM-390 spectrometers and referenced to residual protio solvent. EPR spectra were obtained on a Varian E-Line Century Series spectrometer operating at X-band ($\nu \approx 9.27$ GHz). EPR samples were prepared in either 2-MTHF (vacuum transferred from sodium benzophenone ketyl) or propylene glycol (dried over Na_2SO_4, then distilled under partial vacuum/argon) in the strict absence of oxygen. A liquid nitrogen-filled finger dewar was employed for the 77 K experiments. Variable temperature control in EPR experiments was achieved with a ^{4}He-cooled Oxford Instruments ESR-900 cryostat. The filtered (307–386-nm pass), focused output of either a 1000-W Hg–Xe arc lamp or a 500-W Hg arc lamp was used for photolysis of samples in the EPR cavity. Lamps, housings, lenses, and power supplies were obtained from Oriel Corporation, Stamford, CT. Filters were obtained from Schott Optical Glass Company, Duryea, PA.

Cyclopentadienylmagnesium bromide–THF complex (CpMgBr·THF$_n$) was prepared according to the procedure of Stille and Grubbs.[19] The effective molecular weight of this white solid complex was found to be ca. 400 g/mol by NMR integration against a mesitylene standard.

Bisfulvene 10.[18a] 1,3-Diacetylbenzene (2.52 g, 15.5 mmol), cyclopentadiene (7 mL, 85.4 mmol), and methanol (40 mL) were combined in a 100-mL round-bottomed flask. Pyrrolidine (4.2 mL, 50.3 mmol) was added dropwise and the mixture stirred at room temperature for 30 h. The reaction was quenched by dropwise addition of glacial acetic acid (3 mL). The solvent was removed by rotoevaporation and the residue partitioned between ether (200 mL) and water (100 mL). The aqueous phase was saturated with NaCl and extracted with ether (2 × 100 mL). The combined organics were washed with water (100 mL) and saturated aqueous NaCl (50 mL), dried over $MgSO_4$, and filtered. The solvent was removed by rotoevaporation and the residue chromatographed on silica gel (20% ether/petroleum ether). The first-eluted orange band provided **12** as an orange solid (2.04 g, 51%): ^{1}H NMR (CDCl$_3$) δ 2.50 (s, 6 H), 6.10–6.25 (m, 2 H), 6.35–6.70 (m, 6 H), 7.35 (s, 4 H).

Preparation of 12–13 with CpLi/BF$_3$·Et$_2$O. Cyclopentadienyllithium (16.1 g, 200 mmol) was dissolved in 500 mL of THF and the mixture cooled to –78 °C. Boron trifluoride etherate (25 mL, 203 mmol) was added via cannula and the mixture stirred at –78 °C for 30 min. A solution of **11** (7.0 g, 50 mmol) in THF (150 mL) was added via cannula. The mixture was stirred for 15 min at –78 °C, and then the cooling bath was removed. The mixture was allowed to warm to room temperature and stirred for 40 h and was then poured into 600 mL of saturated aqueous NH$_4$Cl. The organic layer was separated, dried over $MgSO_4$, and filtered, and the solvent was removed by rotary evaporation. Chromatography on silica gel with 10% benzene/petroleum ether provided bisfulvene **13** (243 mg, 2%): ^{1}H NMR (GX-400, CDCl$_3$) δ 1.69 (s, 12 H), 6.39 (d, $J = 4$ Hz, 4 H), 6.50 (d, $J = 4$ Hz, 4 H); ^{13}C NMR (GX-400, CDCl$_3$) δ 30.03, 120.21, 130.95, 137.42, 171.79. Increasing the polarity to 100% benzene gave **12** (4.8 g, 50%): ^{1}H NMR (GX-400, CDCl$_3$) δ 1.50 (s, 12 H), 6.38 (d, $J = 4$ Hz, 2 H), 6.52 (d, $J = 4$ Hz, 2 H).

Conversion of 12 to 13 with CpMgBr. **12** (1.36 g, 7.2 mmol) and CpMgBr (7.2 g, 18 mmol) were refluxed in dioxane for 3 h. The reaction mixture was filtered to remove magnesium salts, which were washed well with ether, and the organic layer was washed with saturated aqueous NH$_4$Cl and dried over $MgSO_4$. Filtration and removal of solvent left 2.5 g of brown residue, which was chromatographed on silica gel using 10% benzene/petroleum ether as eluent to yield **13** (80 mg, 3.6%).

Preparation of 15–16 with CpLi/BF$_3$·Et$_2$O. Cyclopentadiene (9 mL, 110 mmol) was dissolved in 150 mL of tetrahydrofuran and the solution cooled in an ice bath. A solution of *n*-butyllithium in hexanes (32 mL, 2.5 M, 80 mmol) was added over a period of 10 min to yield a milky white slurry. BF$_3$·Et$_2$O (10 mL, 80 mmol) was added to the stirred, cooled slurry over 1 min via syringe. The mixture turned clear and orange upon complete addition. Solid **14** (2.5 g, 20 mmol) was then added, causing the color to become very dark orange. The mixture was stirred for 15 min and then poured into water (200 mL). This mixture was saturated with sodium chloride and extracted with portions of ether (100 mL) until no more color entered the organic phase. The combined organic extracts were dried over $MgSO_4$. The treatment with $MgSO_4$ turned the color of the solution from brown to orange. Filtration and

(30) Jacobs, S. J.; Dougherty, D. A. Manuscript in preparation.

(31) There are exceptions; see, for example: Dvolaitzky, M.; Chiarelli, R.; Rassat, A. *Angew. Chem., Int. Ed. Engl.* **1992**, *31*, 180.

(32) Platz, M. A.; Senthilnathan, V. P.; Wright, B. B.; McCurdy, C. W., Jr. *J. Am. Chem. Soc.* **1982**, *104*, 6494–6501.

(33) Still, W. C.; Kahn, M.; Mitra, A. *J. Org. Chem.* **1978**, *43*, 2923.

removal of solvent gave a residue which was chromatographed on silica gel. Gradient elution (5–20% ether/petroleum ether) gave bisfulvene **16** (600 mg, 14%) as the first yellow band: ^{1}H NMR (GX-400, CDCl$_3$) δ 1.82 (s, 6 H), 3.16 (s, 4 H), 6.45 (m, 2 H), 6.54 (m, 2 H), 6.68 (m, 2 H); ^{13}C NMR (GX-400, CDCl$_3$) δ 32.00, 33.40, 49.99, 119.81, 122.68, 129.45, 131.91, 137.88, 167.74; MS (70 eV EI) *m/z* 222 (M$^+$), 207 (base peak), 192, 165. The second yellow band eluted was keto fulvene **15** (1.1 g, 32%): MS (70 eV EI) *m/z* 174 (M$^+$, base peak), 131, 117.

Bisfulvene 16 from Monofulvene 15. Compound **15** obtained above (1.1 g, 6.3 mmol) was refluxed in 100 mL of tetrahydrofuran with CpMgBr·THF$_n$ (4.9 g, 12 mmol) for 4 h and then stirred overnight at room temperature. The reaction mixture was poured into water (200 mL). The mixture was saturated with NaCl and extracted with portions of ether (100 mL) until no more color entered the organic layer. The combined organic layers were dried over MgSO$_4$, filtered, rotoevaporated, and chromatographed on silica gel. Gradient elution (0–3% ether/petroleum ether) allowed separation of **16** (200 mg, 14%).

TMS Ether 17. 2-Hydroxy-9-adamantanone^{22} (13.8 g, 83 mmol) was suspended in hexane, and trimethylsilyl chloride (3.7 mL, 29.1 mmol) and hexamethyldisilazane (6.1 mL, 29.1 mmol) were added via syringe. The reaction was monitored by TLC (2% methanol/methylene chloride). After 12 h, the reaction mixture was filtered and concentrated to give **17** as a white solid (17.5 g, 89%), which was used without purification: MS (70 eV EI) *m/z* 237 (M$^+$), 223 (base peak).

Fulvene 18. Adamantanone TMS ether **17** (4.77 g, 20 mmol) was added to a tetrahydrofuran solution of CpMgBr·THF$_n$ (12 g, ca. 30 mmol), and the solution was brought to reflux. The reaction was monitored by TLC (2:1 petroleum ether/ether). After 18 h, the reaction mixture was cooled to room temperature, poured onto cracked ice, and diluted with ether. The resulting mixture was washed with saturated NH$_4$Cl (2 × 100 mL) and saturated aqueous NaCl (2 × 100 mL). The organic phase was dried with MgSO$_4$ and concentrated. The bright yellow residue was chromatographed on silica gel (4:1 petroleum ether/ether). First yellow band was collected and evaporated to give 4.1 g (71%) of **18**: MS (70 eV EI) *m/z* 286 (M$^+$), 73 (base peak). The second band proved to be the alcohol **19** (1.0 g, 21%): MS (70 eV EI) *m/z* 214 (M$^+$).

Alcohol 19. Compound **18** (4.1 g, 14 mmol) was dissolved in 50 mL of acetonitrile. Triethylamine tris(hydrofluoride)^{34} (4.7 mL, 28 mmol) was added via syringe. The reaction was complete within 30 min as judged by TLC (2:1 petroleum ether/ether)). The reaction mixture was diluted with 100 mL of ether and poured into a separatory funnel containing 200 mL of saturated NH$_4$Cl. The layers were separated, and the organic layer was washed with water (2 × 150 mL), saturated NaHCO$_3$, and saturated NaCl. The solution was dried with MgSO$_4$ and concentrated to give 2.9 g (95%) of **19** as a bright yellow solid, which was used immediately in the next step.

Keto Fulvene 20 by Swern Oxidation.^{35} Freshly distilled oxalyl chloride (1.3 mL, 14.9 mmol) was added to anhydrous DMSO (2.1 mL, 29.7 mmol) dissolved in 50 mL of dry methylene chloride at −78 °C. The mixture was stirred for 15 min, and a methylene chloride solution of **19** (2.9 g, 13.5 mmol) was added over 10 min. After the mixture was stirred for 1 h at −78 °C, freshly distilled triethylamine (10 mL, 68 mmol) was added, and the reaction mixture was warmed to room temperature. The reaction mixture was filtered to remove insoluble salts (Et$_3$NHCl) and was washed with saturated aqueous NH$_4$Cl (3 × 100 mL) and saturated aqueous NaCl (2 × 100 mL). The organic phase was dried with MgSO$_4$ and concentrated to give 2.7 g (93%) of bright yellow crystals. The product was analyzed by GC/MS and used immediately in the next step: MS (70 eV EI) *m/z* 212 (M$^+$, base peak).

Bisfulvene 21. Crude ketone **20** (2.7 g, 12.7 mmol) and a THF solution of CpMgBr·THF$_n$ (7.7 g, 19.1 mmol) were heated to reflux. The reaction was followed by TLC (2:1 petroleum ether/ether). After 22 h, the reaction mixture was cooled to room temperature, poured onto cracked ice, and diluted with ether. The resulting mixture was washed with saturated NH$_4$Cl (2 × 100 mL) and saturated NaCl (2 × 100 mL). The organic phase was dried with MgSO$_4$ and concentrated to yield 1.8 g (53%) of bright yellow crystals of bisfulvene **21**: ^{1}H NMR (QE-300, CDCl$_3$) δ 2.04–2.18 (m, 9 H), 3.38 (bs, 2 H), 4.59 (bs, 1 H), 6.48–6.55 (m, 6 H), 6.55 (m, 2 H); ^{13}C NMR (QE-300, CDCl$_3$) δ 28.3, 36.7, 39.3, 40.8, 43.0, 45.9, 119.2, 119.9, 131.3, 131.5, 136.7, 161.7; MS (70 eV EI) *m/z* 260 (M$^+$).

Fulvene 29. This compound was prepared using the procedure for bisfulvene **10**:^{18a} ^{1}H NMR (QE-300, CDCl$_3$) δ 1.85–2.15 (m, 12 H), 3.29 (bs, 1 H), 6.58 (m, 4 H); ^{13}C NMR (QE-300, CDCl$_3$) δ 28.12,

36.86, 37.15, 40.06, 119.27, 130.29, 135.65, 167.03; MS (70 eV EI) *m/z* 198 (M$^+$).

Preparation of Reduced Diels–Alder Adducts: Representative Procedure.^{18b} Bisfulvene **16** (140 mg, 0.63 mmol) was treated with dimethyl azodicarboxylate (DMAD, 184 mg, 1.26 mmol) in methylene chloride (20 mL) at room temperature and the mixture allowed to stand for 15 min. The mixture was cooled in an ice bath, and stirring was begun as solid potassium azodicarboxylate (1.22 g, 6.3 mmol) was added. A solution of acetic acid (0.72 mL, 12.6 mmol) in methylene chloride (5 mL) was added dropwise over 0.5 h. Stirring was continued overnight as the ice bath warmed. The reaction was quenched by the addition of water (10 mL). Additional methylene chloride (25 mL) was added, and the mixture was separated. The aqueous phase was extracted with methylene chloride (2 × 25 mL), and the combined organics were dried over anhydrous K$_2$CO$_3$. Filtration, removal of solvent, and chromatography (75% ethyl acetate/petroleum ether) allowed isolation of the white solid product isomeric tetrakiscarbamates **27** (163 mg, 46%).

Data for compounds prepared in this fashion follow.

25: ^{1}H NMR (EM-390, CDCl$_3$) δ 1.5–2.0 (bs, 8 H), 2.10 (s, 6 H), 3.67 (s, 6 H), 3.75 (s, 6 H), 4.60 (bs, 2 H), 4.90 (bs, 2 H), 7.00 (d, *J* = 5 Hz, 2 H), 7.10 (s, 1 H), 7.30 (t, *J* = 5 Hz, 1 H); HRMS (M$^+$) calcd for C$_{28}$H$_{34}$N$_4$O$_8$ 554.2377, obsd 554.2379.

26: ^{1}H NMR (GX-400, CDCl$_3$) δ 1.20 (s, 12 H), 1.80 (m, 4 H), 2.05 (m, 4 H), 2.95 (s, 6 H), 4.68 (s, 4H).

27: ^{1}H NMR (EM-390, CDCl$_3$) δ 1.21 (overlapping s & d, 6 H), 1.70 (bs, 4 H), 2.38 (bs, 4 H), 3.65 (bs, 12 H), 4.56 (bs, 2 H), 4.94 (bs, 2 H); HRMS (MH$^+$) calcd for C$_{25}$H$_{35}$N$_4$O$_8$ 519.2455 obsd 519.2482.

28: ^{1}H NMR (EM-390, CDCl$_3$) δ 1.2 (m, 4 H), 1.4–2.2 (m, 13 H), 2.65 (bs, 2 H), 3.40 (bs, 1 H), 3.75 (bs, 12 H), 4.80 (bs, 4 H); HRMS (M$^+$) calcd for C$_{28}$H$_{36}$N$_4$O$_8$ 556.2533, obsd 556.2532.

30: ^{1}H NMR (EM-390, CDCl$_3$) δ 1.0–2.0 (m, 16 H), 2.5 (bs, 2 H), 3.6 (bs, 6 H), 4.7 (bs, 2 H); MS (70 eV EI) *m/z* 346 (M$^+$), 198 (base peak).

Note: Due to slow rotation of the amide linkages, ^{13}C NMR spectra of these compounds taken in CDCl$_3$ displayed poor resolution up to 50 °C, and thus, only ^{1}H NMR spectra are reported. These compounds were also characterized by exact mass analysis. The corresponding bisdiazenes were characterized by ^{13}C and ^{1}H NMR (see below).

Preparation of Bisdiazenes: Representative Procedure. Compound **25** (275 mg, 495 μmol) was heated to reflux for 2 h with 85% KOH (1.0 g) in Ar-purged 2-propanol (10 mL). The mixture was allowed to cool to room temperature, and solid NaHCO$_3$ (2.0 g) was added. After the mixture was stirred overnight at room temperature, the 2-propanol was removed under high vacuum. Water (25 mL) was added, and the aqueous phase was extracted with methylene chloride (3 × 25 mL). The brown solution of hydrazine was dried over Na$_2$SO$_4$, decanted, and cooled to 0 °C. Nickel peroxide (1.0 g) was added, and the mixture was stirred for 1 h at 0 °C. Filtration through Celite and removal of solvent provided **1**-(N$_2$)$_2$ (130 mg, 82%).

Data for bisdiazenes follow.

1-(N$_2$)$_2$: ^{1}H NMR (QE-300, CDCl$_3$) δ 1.05–1.30 (m, 4 H), 1.65–1.81 (m, 4 H), 2.00 (2s, 6 H), 5.23 (m, 2 H), 5.48 (d, *J* = 2.3 Hz, 2 H), 6.82 (m, 1 H), 7.00 (m, 2 H), 7.27 (t, *J* = 7.7 Hz); ^{13}C NMR (QE-300, CDCl$_3$) δ 19.81, 21.05, 21.10 ,21.27, 21.29, 74.35, 74.43, 74.50, 124.51, 124.55, 126.20, 126.25, 126.37, 126.41, 128.03, 140.61, 141.81; UV λ_{max} = 342 nm.

2-(N$_2$)$_2$ (syn isomer only): ^{1}H NMR (QE-300, CDCl$_3$) δ 1.05 (m, 4 H), 1.23 (s, 12 H), 1.62 (m, 4 H), 5.25 (s, 4H); ^{13}C NMR (QE-300, CDCl$_3$) δ 21.29, 21.33, 26.55, 27.47, 28.40, 46.52, 73.77, 73.82, 134.82, 142.59; UV λ_{max} = 342 nm.

3-(N$_2$)$_2$ (syn and anti isomers): ^{1}H NMR (QE-300, CDCl$_3$) δ 1.10 (m, 4 H), 1.21 (s) and 1.23 (d, *J* = 5 Hz) (6 H total), 1.63 (m, 4 H), 2.31 (m, 4 H), 5.57 (s, 2 H), 5.24 and 5.25 (2 overlapping s, 2 H); ^{13}C NMR (QE-300, CDCl$_3$) δ 20.86, 20.91, 21.36, 28.42, 28.99, 29.46, 29.54, 29.65, 45.32, 45.35, 72.44, 72.48, 75.95, 76.00, 135.38, 139.20; UV λ_{max} = 342 nm.

4-(N$_2$)$_2$: ^{1}H NMR (QE-300, CDCl$_3$) δ 1.0–1.18 (m, 4 H), 1.38–1.5 (m, 4 H), 1.58–2.0 (m, 8 H), 2.56 (s, 2 H), 3.14 (s, 1 H), 5.28–5.41 (m, 4 H); ^{13}C NMR (QE-300, CDCl$_3$) δ 21.22, 21.18, 21.28, 21.32, 21.40, 27.68, 27.71, 34.13, 34.24, 37.29, 37.64, 38.05, 39.84, 39.94, 39.99, 40.83, 41.04, 72.62, 72.77, 73.02, 73.10, 73.15, 131.75, 131.83, 132.27, 133.27, 134.14, 134.24; UV λ_{max} = 342 nm.

31: ^{1}H NMR (QE-300, CDCl$_3$) δ 1.07 (m, 2 H), 1.55–1.89 (m, 14 H), 2.53 (bs, 2 H), 5.38 (s, 2 H); ^{13}C NMR (QE-300, CDCl$_3$) δ 21.47, 27.92, 28.09, 34.54, 36.75, 38.42, 39.31, 73.07, 130.85, 136.02; UV λ_{max} = 342 nm.

Calculations on Trimethylene in Adamantane Geometry. The structure of bisfulvene **21** was energy minimized with the MM2 force field as implemented in Macromodel. The geometry of the C8–C1–C2 fragment thus obtained was frozen, and all the carbon atoms were replaced by

(34) Nyström, J.-E.; McCanna, T. D.; Helquist, P.; Iyer, R. S. *Tetrahedron Lett.* **1985**, *26*, 5393.

(35) Omura, K.; Swern, D. *Tetrahedron* **1978**, *34*, 1651. Mancuso, A. J.; Huang, S. L.; Swern, D. *J. Org. Chem.* **1978**, *43*, 2480.

hydrogen atoms while maintaining the bond and dihedral angles, but shortening the bond lengths to 1.10 Å. The coordinates of this trimethylene were then submitted to Gaussian 90 for single–point calculations using the D95V basis set (Dunning's basis set). The GVB(1/2) singlet energy was –116.955 578 9 hartrees, and the ROHF triplet energy was –116.953 473 4 hartrees, indicating a singlet ground state and a singlet–triplet gap of 1.3 kcal/mol.

Matched OD Photolysis of 4-(N$_2$)$_2$ and 31. MTHF solutions of 4-(N$_2$)$_2$ with A(342 nm) = 1.4 and **31** with A(342 nm) = 1.3 were prepared. The solutions were pipetted into quartz EPR tubes fitted with vacuum stopcocks and submitted to five freeze–pump–thaw cycles. Samples were irradiated sequentially at 50 K using the same source and filter combination. Plots of signal intensity vs photolysis time are shown in Figure 7.

Variable-Temperature EPR Study of 3. An EPR sample of **3**-(N$_2$)$_2$ in 1,2-propanediol was photolyzed for 6 h at 50 K. The temperature was raised briefly (~5 min) to 120 K in order to anneal the sample, and spectra were taken at decreasing temperatures down to 10 K.

Simulation of EPR Spectra. We modified a published procedure[26] for the computation of EPR powder spectra. The EPR spin Hamiltonian used is shown in eq 6, shown again here for convenience.

$$\hat{H} = g\beta\mathbf{B}\cdot\hat{S} + D(\hat{S}_z^2 - (S(S+1)/3)) + E(\hat{S}_x^2 - \hat{S}_y^2) \qquad (6)$$

The expression for the first-derivative powder spectrum is[26,36,37]

$$\frac{\partial I}{\partial B} = \sum_{i<j} \int_0^{\pi/2} \int_0^{\pi/2} \langle V_{ij}\rangle \frac{\partial B}{\partial v} \frac{\partial}{\partial B}\left(\frac{1}{(2\pi)^{1/2}\sigma_{ij}} e^{-1/2[(B-B_0)/\sigma_{ij}]^2}\right) \sin\theta \; d\theta \; d\phi \qquad (13)$$

(36) Aasa, R.; Vänngård, T. *J. Mag. Res.* **1975**, *19*, 308.
(37) van Veen, G. *J. Magn. Reson.* **1978**, *91*, 30.

Numerical integration of eq 13 was required in order to simulate spectra. Parameters θ and ϕ were varied in 1° increments between 0° and 90°. At each orientation, the resonant fields for each of the Δm_s = 1 and Δm_s = 2 transitions were computed by solving the resonance condition $E_i - E_j = g\beta B$ by interative diagonalization of the Hamiltonian matrix of eq 1. Once the resonance field was found for a given transition, the eigenvectors $|i\rangle$ and $|j\rangle$ belonging to the two energy eigenvalues E_i and E_j were computed as linear combinations of the $\hat{S}_z$ basis functions. The transition probability could then be calculated according to eq 14.[26,37,38] The

$$\langle V_{ij}\rangle = \frac{\pi g^2\beta^2 B_1}{2}\left[|\langle i| \cos\theta \cos\phi \; \hat{S}_x + \cos\theta\sin\phi \; \hat{S}_y + \sin\theta \; \hat{S}_z|j\rangle|^2 + |\langle i| \sin\phi \; \hat{S}_x - \cos\phi \; \hat{S}_y|j\rangle|^2\right] \qquad (14)$$

derivative $\partial B/\partial v$ was approximated as $h/g\beta\Delta m_s$.[36,39] Powder spectra were obtained in final form by fitting a Gaussian line shape to the single transitions computed above and summing over all transitions. Line widths in powder EPR spectra are orientation-dependent; thus the line width was represented as a diagonal tensor σ.[26,38,39] The width of the Gaussian applied to a given transition was determined from eq 15.[26]

$$\sigma_{ij}^2 = (\cos\theta\cos\phi \; \sigma_{xij})^2 + (\cos\theta\sin\phi \; \sigma_{yij})^2 + (\sin\theta \; \sigma_{zij})^2 \qquad (15)$$

(38) Wasserman, E.; Snyder, L. C., Yager, W. A. *J. Chem. Phys.* **1964**, *41*, 1763.
(39) Kottis, P.; Lefebvre, R. *J. Chem. Phys.* **1964**, *41*, 379.

Molecular Solid-State Organometallic Chemistry of Tripodal (Polyphosphine)metal Complexes. Catalytic Hydrogenation of Ethylene at Iridium

Claudio Bianchini,*,† Erica Farnetti,‡ Mauro Graziani,*,‡ Jan Kaspar,‡ and Francesco Vizza†

Contribution from the Istituto per lo Studio della Stereochimica ed Energetica dei Composti di Coordinazione, CNR, Via J. Nardi 39, 50132 Firenze, Italy, and Dipartimento di Scienze Chimiche, Università di Trieste, Via Valerio 38, 34127 Trieste, Italy. Received March 27, 1992

Abstract: The solid–gas reactions of [(triphos)Ir(H)$_2$(C$_2$H$_4$)]BPh$_4$ (**1**) with CO, C$_2$H$_4$, and H$_2$ are described [triphos = MeC(CH$_2$PPh$_2$)$_3$]. The gaseous reactants promote the elimination of ethane from **1** and the formation of [(triphos)Ir(CO)$_2$]BPh$_4$, [(triphos)Ir(C$_2$H$_4$)$_2$]BPh$_4$, and [(triphos)Ir(H)$_2$]BPh$_4$, respectively. The latter 16-electron species is isolable in the solid state at temperatures <70 °C. At higher temperatures, [(triphos)Ir(H)$_2$]$^+$ dimerizes in the solid state to give the tetrahydride [(triphos)HIr(μ-H)$_2$HIr(triphos)]$^{2+}$. Dimerization is avoided when the unsaturated fragment is incorporated into the lattice of a polyoxometalate cluster such as PW$_{12}$O$_{40}$$^{3-}$. The complex [(triphos)Ir(H)$_2$(C$_2$H$_4$)]BPh$_4$ is an effective catalyst for the hydrogenation of ethylene in the solid state at 60 °C. Comparisons are made with analogous fluid solution-phase systems.

Molecular solid-state organometallic chemistry is experiencing rapid growth through the reactions of materials derived from either metal oxide clusters of the Keggin-ion type[1] or tripodal polyphosphine ligands.[2]

We are developing the solid-state chemistry of Group VIII metal complexes stabilized by tripodal polyphosphines such as P-(CH$_2$CH$_2$PPh$_2$)$_3$ (PP$_3$), N(CH$_2$CH$_2$PPh$_2$)$_3$ (NP$_3$), and MeC-(CH$_2$PPh$_2$)$_3$ (triphos) (Scheme I).

Scheme I
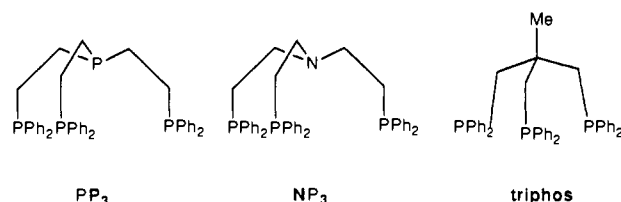
Earlier work has shown that (i) the Co(I) complex [(PP$_3$)-Co(N$_2$)]BPh$_4$ (**1**) reacts in the solid state with a variety of gaseous

†CNR, Florence.
‡University of Trieste.